Caspian Journal of Environmental Sciences
Online ISSN: 1735-3866
Print ISSN: 1735-3033

Sustainable dehydration of Sary Irimshik, a layered-porous fermented dairy product: Comparative kinetics and energy efficiency of convective and infrared drying

Mariam Alimardanova, Kanash Kuzembayev, Gaukhar Kuzembayeva, Dinara Tlevlessova*

Almaty Technological University, Tole bi av, 100, Almaty, Kazakhstan

* *Corresponding author's E-mail: tlevlessova@gmail.com*

ABSTRACT

Sary Irimshik is a traditional layered-porous fermented dairy product whose dehydration behaviour has not previously been characterized in detail, despite its relevance for energy-efficient and microbiologically safe processing of regional dairy resources. Convective (50-55 °C, 0.5-2.0 m s^{-1}, 5-10 mm layer) and infrared (40-60 °C, 5-10 mm layer) drying were studied at two processing stages of the product, a raw curd (initial moisture 70.2%) and a pressed semi-product (initial moisture 33.0%). The resulting kinetics were fitted with the Page and Fick models, and water activity, moisture binding energy and an engineering heat balance for a 10 kg infrared-dryer batch were additionally determined. Drying proceeded entirely in the falling-rate period in all series, with the Page model exponent n ranging from 1.51 to 1.85 for convective drying and from 1.44 to 1.50 for infrared drying (R^2 = 0.992-0.998), outperforming the Fick model (R^2 = 0.897) because the effective diffusion coefficient increased from 3.5×10^{-11} to 3.3×10^{-10} m^2 s^{-1} as drying progressed rather than remaining constant. Water activity declined from 0.45 to 0.20 while moisture binding energy rose from 1.95 to 3.92 kJ mol^{-1} as moisture content fell from 33 to 15%. Infrared drying halved the processing time relative to convective drying (240 versus 480 min) and required about 1.0 kW of thermal power for a 10 kg batch, at a specific heat consumption of 4.24 MJ per kilogram of evaporated water. These findings agree with reports for other diffusion-limited, protein-rich food matrices and indicate that infrared, or combined infrared-convective, drying provides a more energy-efficient and microbiologically safer dehydration route than conventional convective drying for Sary Irimshik and structurally similar dairy products. Infrared-assisted drying is recommended for scale-up trials, together with further work to separate the effect of heating mode from sample geometry on the kinetic exponent.

Keywords: Drying kinetics, Effective diffusivity, Infrared drying, Page model; Sary Irimshik, Water activity.
Article type: Research Article.

INTRODUCTION

Dried fermented dairy products are among the most technologically challenging drying objects, because the process is governed not only by the structural and mechanical properties of the material but also by a complex set of physicochemical and biochemical transformations that accompany moisture removal. Sary Irimshik is a traditional fermented dairy product obtained from cow and goat milk by an acid-rennet method. During processing it develops a layered, protein-capillary porous structure that differs substantially from the relatively homogeneous casein matrix of conventional cheese systems. This structural feature produces heterogeneous interlayer moisture-retention zones and, consequently, a specific drying kinetics that merits dedicated study. Sary Irimshik belongs to a broad family of traditional dried fermented dairy products of Central Asia (kurut, kurt, and kashk), which have so far been studied mainly from the standpoint of starter-culture microbiology and recipe modification (Tuganbay

Caspian Journal of Environmental Sciences, Vol. 24 No. 4 pp.1177-1189 Received: Jan. 15, 2026 Revised: April 09, 2026 Accepted: May 20, 2026
DOI: 10.22124/cjes.2026.10050
© The Author(s)
Publisher: University of Guilan

et al. 2022; on kurut fermented with a probiotic *Lacticaseibacillus rhamnosus* GG strain; Kalibekkyzy *et al.* 2026; on kurt enriched with dairy and plant by-products). However, the engineering aspects of heat and mass transfer during drying of this product group, including kinetic models and moisture diffusion coefficients, have not been systematically addressed in the accessible literature, which motivates the present study. Analysis of the literature on drying of fermented dairy products shows that convective drying in tray dryers and infrared (radiant) drying are the most technologically and economically justified intensification methods, owing to their ease of scale-up and moderate energy requirements compared with freeze-drying and other specialized techniques (Aboud *et al.* 2019; Salehi 2020). The present study continues a series of works by the author team on traditional and functional fermented dairy products of Kazakhstan: comparative characteristics of goat and cow milk products from different regions of the country (Alimardanova *et al.* 2022), the effect of enterosorbing dietary fibres on the quality and safety of fermented milk products (Alimardanova & Bakiyeva 2022), technology of functional fermented milk products with plant additives (Alimardanova *et al.* 2022), and comparative kinetic modelling of Ayran fermentation with functional additives (Alimardanova *et al.* 2026). The use of two empirical models (Page and Fick) to describe mass-transfer kinetics in the present work is methodologically consistent with the kinetic-modelling approach applied in the latter study, ensuring continuity of methods within this research program. The aim of this study was to investigate the moisture behaviour of Sary Irimshik during convective and infrared drying, to develop a mathematical description of the dehydration kinetics, and to provide an engineering justification for a rational, more sustainable and energy-efficient drying method for this traditional dairy product.

To achieve this aim, the following objectives were addressed (the section reporting the corresponding result is indicated in parentheses):

(1) reviewing the literature to justify the choice of drying methods;

(2) characterizing the layered-porous structure and identify the forms of moisture retention at successive stages of dehydration;

(3) determining the change in water activity and moisture binding energy with decreasing moisture content;

(4) experimentally investigating the convective drying kinetics of the product at two processing stages, a raw curd and a pressed semi-product;

(5) developing a mathematical description of the drying kinetics based on the Page and Fick models and evaluating their adequacy;

(6) performing an analytical critical-point analysis of the drying curve;

(7) investigating the kinetics of infrared drying;

(8) comparing convective and infrared drying in terms of duration, energy consumption and kinetic indices;

(9) performing an engineering heat-balance calculation for an infrared dryer;

and (10) providing an engineering justification for a rational drying method.

Scientific novelty

A comprehensive characterization of the layered protein-capillary porous structure of sary irimshik as a drying object is provided for the first time, identifying four forms of bound moisture (free, capillary-bound, osmotically bound and adsorption-bound) and their correspondence to successive drying stages.

Quantitative data on the change in water activity (from 0.45 to 0.20) and moisture binding energy (from 1.95 to 3.92 kJ mol^{-1}) during drying of this product are reported for the first time.

The absence of a constant-rate period is established: the process is diffusion-limited from the outset, which distinguishes Sary Irimshik from a number of classical drying objects.

A joint comparison of the empirical Page model and the diffusional Fick model is performed, including calculation of the effective diffusion coefficient Deff and demonstration of its variation with time, which explains the superiority of the nonlinear model.

An analytical critical-point analysis of the drying curve is applied for the first time to this product, by differentiating the Page-model function to obtain the inflection point, critical moisture content and maximum drying rate.

The Page-model nonlinearity exponents for convective ($n = 1.51$-1.85) and infrared ($n \approx 1.44$-1.50) drying of the same product are quantitatively compared as an objective indicator of mass-transfer intensification.

Practical significance

Process parameters for convective (50-55 °C, 0.5-2.0 m s^{-1}, 5-10 mm layer) and infrared (40-60 °C, 100 mm emitter distance) drying are established for use in production regulations.

A predictive mathematical model of moisture content over time is developed, enabling rational drying duration to be calculated and both under- and over-drying to be avoided.
An engineering heat-balance calculation is performed that is directly applicable to the selection or design of laboratory- and small-industrial-scale infrared drying equipment.
Infrared (or combined infrared-convective) drying is recommended as a more energy-efficient and quality-preserving dehydration method, supporting more sustainable processing of this traditional dairy resource.

MATERIALS AND METHODS

Object of study

Sary Irimshik obtained from cow and goat milk by an acid-rennet method was used as the object of study. Two processing stages of the product were considered: (A) a raw curd immediately after acid-rennet coagulation and concentration of the milk mass, characterized by a high initial moisture content, and (B) a semi-product after removal of free whey and formation of a uniform layer of a set thickness (5-10 mm), used in most of the regime experiments. Semi-product (B) characteristics: moisture content 30-35%, protein 14-18%, fat 5-9%, acidity 180-220 °T, uniform granular consistency. The use of a mixed cow-and-goat milk raw material is consistent with previously reported regional differences in the composition and properties of goat and cow fermented dairy products in farms of the Akmola and North Kazakhstan regions (Alimardanova & Shunekeyeva 2022), which was taken into account when selecting and standardizing the raw-material batches for the present experiment.

Convective drying set-up

Convective drying was carried out on a laboratory rig comprising a drying chamber with electric heaters, a sample pan, a balance, and a control panel with a multiplexer recording chamber temperature (T), sample temperature (T0), sample mass (M), inlet air humidity (Wn), and consumed electric power (N). The current sample mass was recorded continuously, with automatic conversion of the absolute moisture loss into relative indices. The regime parameters of convective drying are given in Table 2.

Table 1. Characteristics of Sary Irimshik at the two processing stages studied.

Parameter	Raw curd (Series A)	Pressed semi-product (Series B)
Initial moisture content W0 (%)	70.2	33.0 (32-35)
Equilibrium moisture content We (%)	15.0	15.0 (Xe = 0.1765 kg kg^{-1})
Layer thickness, mm	-	5-10
Protein content (%)	-	14-18
Fat content (%)	-	5-9
Acidity (°T)	-	180-220

Table 2. Convective drying regimes of Sary Irimshik.

Parameter	Value
Air temperature (°C)	50-55
Air velocity (m s^{-1})	0.5-2.0
Layer thickness (mm)	5-10
Sample mass (g)	50-200
Final moisture content (%)	15-17

Infrared drying set-up

Infrared drying was carried out on a batch laboratory unit comprising a heat-insulated chamber, ceramic/quartz infrared emitters, a sample tray, thermal sensors and a balance for recording the current mass. The distance between the emitter and the product surface was 100 mm. Emitter temperature (40-60 °C) and layer thickness (5 and 10 mm) were varied; moisture content was determined at 20-30 min intervals until a final value of 15-17% was reached. In parallel, rapid moisture determination was carried out using an infrared moisture analyzer of the thermogravimetric type (sample mass 3.0-5.0 g, temperature 105 °C, end criterion: mass change below 1 mg per 30 s).

Mathematical description of drying kinetics

The moisture ratio (MR) was calculated as:

$MR = (W - We) / (W0 - We)$,

where W is the current moisture content (%), W0 the initial moisture content (%), and We the equilibrium moisture content (%). Drying kinetics were described by the empirical Page model:

$MR = \exp(-k \times t^n)$,

where k is the kinetic coefficient and n the nonlinearity exponent. Coefficients were determined by linearization: $\ln(-\ln MR) = \ln k + n \times \ln t$ (the point t = 0 was excluded from the regression). For a physical description of internal mass transfer, the second Fick's law was used in the form of the first-term solution for a flat slab of thickness 2L:

$$MR \approx (8/\pi^2) \times \exp[-\pi^2 \times Deff \times t / (4L^2)],$$

from which the effective diffusion coefficient Deff was obtained from the slope of ln(MR) versus t. Drying rate was calculated from finite differences, $N = (Wi - Wi + 1)/(ti + 1 - ti)$; the critical point (inflection point tcr) of the Page-model drying curve was found analytically from the condition W"(t) = 0: $tcr = [(n-1)/(k \times n)]^{(1/n)}$.

Statistical criteria for model adequacy

Fit accuracy was evaluated using the coefficient of determination (R^2), the root mean square error (RMSE), the mean absolute error (MAE) and the chi-square criterion (χ^2):

$$RMSE = \mathrm{sqrt}[(1/N) \times \Sigma (MRexp - MRmodel)^2]; \quad \chi^2 = \Sigma (MRexp - MRmodel)^2 / MRmodel.$$

This reduced set of criteria (R^2, RMSE, χ^2) is widely used in the current literature on food drying; it has been shown that applying a full set of 13 statistical criteria to evaluate 23 thin-layer drying models gives results statistically consistent with the reduced set of r, R^2, χ^2 and RMSE, which justifies the use of these four indices for engineering calculations (Kilic 2025).

Engineering heat-balance calculation

The heat balance of the infrared drying process was calculated as the sum of the heat required to warm the product, $Q_1 = G0 \times c \times (tk - t0)$, and the heat required to evaporate the moisture, $Q_2 = Gm \times r$, converted to the total heat demand accounting for dryer efficiency, $Qtot = (Q_1 + Q_2)/\eta$. The required thermal power was determined as $N = Qtot/\tau$, and the dryer throughput was calculated with respect to raw material, finished product and evaporated moisture as the corresponding mass divided by the process duration τ.

RESULTS

Forms of bound moisture in the structure of Sary Irimshik

Examination of the product structure at different stages of dehydration identified four forms of moisture retention, distinguished by their binding energy to the matrix and by the conditions under which they are removed during drying (Table 3).

Water activity and moisture binding energy

Water activity (aw) and moisture binding energy were determined at successive levels of moisture content (Table 4, Fig. 1). As moisture content decreased from 33% to 15%, aw decreased monotonically from 0.45 to 0.20, while moisture binding energy increased from 1.95 to 3.92 kJ mol^{-1}.

Table 3. Forms of moisture retention in the structure of Sary Irimshik.

Form of moisture	Location in the structure	Removal characteristics
Free	Interparticle space and large capillaries	Removed at the initial stage
Capillary-bound	Interlayer capillary zones	Removed at a reduced rate
Osmotically bound	Colloidal protein system	Requires increased energy input
Adsorption-bound	Surface of proteins and mineral components	Removed at the final stage

Convective drying kinetics of raw curd (Series A)

Convective drying of the raw curd (W0 = 70.2%) reduced moisture content to 15.2% within 600 min (Table 5, Fig. 2). Linearization of ln (-ln MR) versus ln t gave the equation $\ln(-\ln MR) = -8.0993 + 1.5148 \times \ln t$, i.e. n = 1.5148 and $k = e^{-8.0993} = 0.000304$ (Fig. 3). The resulting Page model for Series A is:

$W(t) = 15.0 + 55.2 \times \exp(-0.000304 \times t^{1.5148})$, $R^2 = 0.9976$.

Table 4. Change in water activity and moisture binding energy of Sary Irimshik with decreasing moisture content.

Moisture content (%)	aw	Moisture binding energy (kJ mol^{-1})
33	0.45	1.95
30	0.38	2.36
27	0.33	2.70
24	0.28	3.10
21	0.24	3.48
18	0.22	3.69
15	0.20	3.92

Table 5. Convective drying kinetics of raw curd (Series A).

t (min)	W (%)	MR
0	70.2	1.0000
60	62.1	0.8533
120	51.3	0.6576
180	40.4	0.4601
240	31.6	0.3007
300	25.3	0.1866
360	21.2	0.1123
420	18.5	0.0634
480	16.8	0.0326
540	15.9	0.0163
600	15.2	0.0036

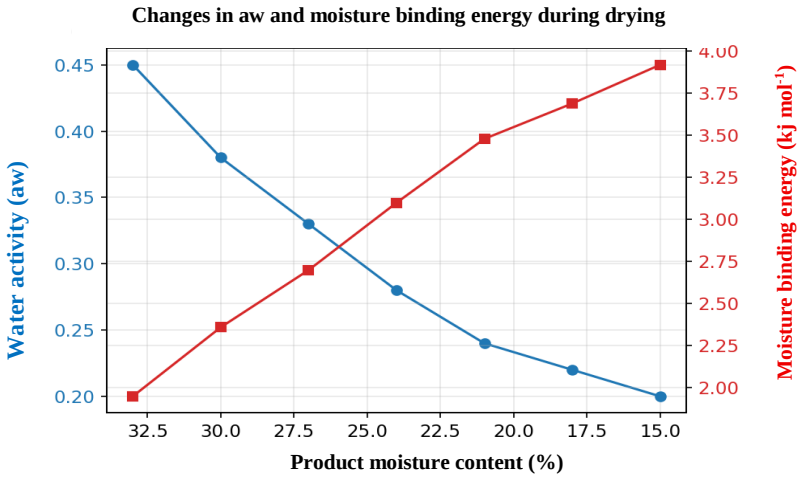

Fig. 1. Changes in water activity (aw) and moisture binding energy during drying of Sary Irimshik.

Convective drying kinetics of the pressed semi-product (Series B) and comparison of the Page and Fick models

For the pressed semi-product (W0 = 33.0%, layer 5-7 mm, agent temperature 50-55 °C, air velocity 0.5 m s^{-1}), moisture content decreased to 15.0% within 480 min (Table 6). Linearization of the Page model gave n = 1.854, $k = 3.78 \times 10^{-5}$; the resulting equation is $MR = \exp(-3.78 \times 10^{-5} \times t^{1.854})$. The effective diffusion coefficient obtained from the linearized Fick solution (layer thickness 2L = 5 mm) was $D_{eff} = 3.57 \times 10^{-10}$ m^2 s^{-1} ($R^2 = 0.897$ for the linearization itself); substituting this value into $k = \pi^2 D_{eff}/(4L^2)$ for n = 1 gives a theoretical $k_{theor} \approx 1.41$

× 10^{-4}, an order of magnitude different from the empirical kexp = 3.78 × 10^{-5}. The two models are compared against the experimental data in Fig. 4, and the corresponding fit statistics are given in Table 7: RMSE = 0.031, χ^2 = 0.073, R^2 = 0.992 for the Page model, versus RMSE = 0.085, χ^2 = 0.215, R^2 = 0.897 for the Fick model with Deff = const. Calculation of the local diffusion coefficient over successive time intervals, Deff(t), showed an increase from about 3.5 × 10^{-11} to about 3.3×10^{-10} m^2 s^{-1} as moisture content decreased.
The drying-rate curve for Series B (Fig. 5) was fitted with the quadratic equation N = -4.713×10^{-4}×W^2 + 0.02275 × W - 0.21986 (R^2 = 0.695), with the maximum rate occurring at W ≈ 25-30%.

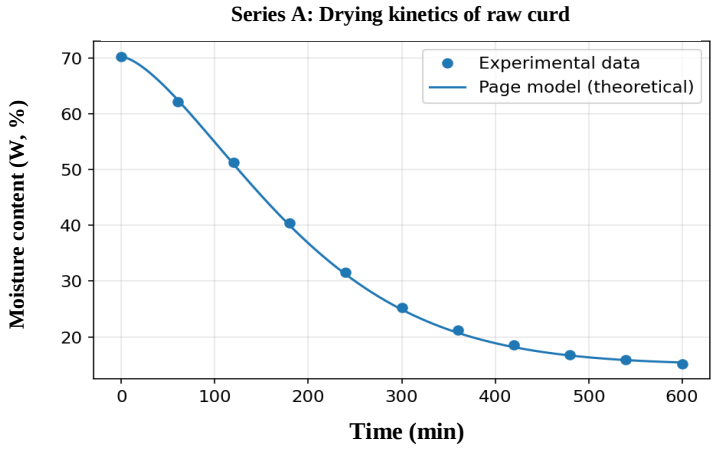

Fig. 2. Drying kinetics of raw curd (Series A) and its fit with the Page model.

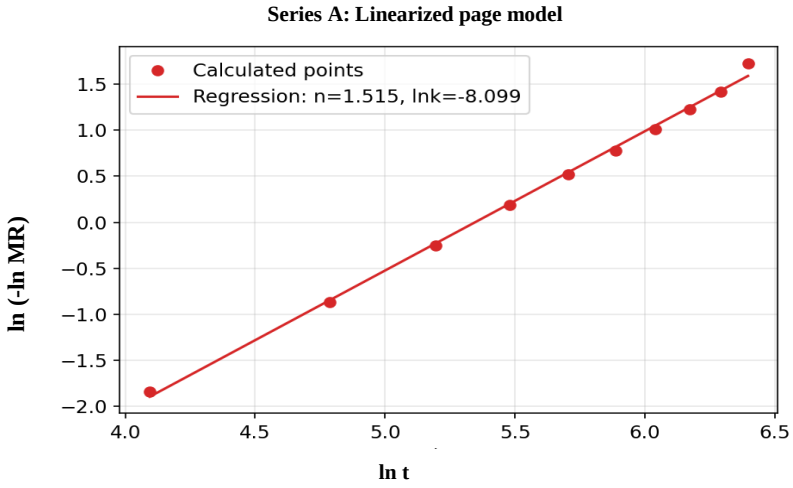

Fig. 3. Linearized Page model for Series A.

Critical-point analysis of the drying curve

For Series A, the inflection point of the function W(t), obtained analytically from the condition W''(t) = 0 using tcr = $[(n-1)/(k\times n)]^{(1/n)}$, was found at tcr ≈ 102.9 min, corresponding to a moisture content Wcr ≈ 54.3% and a maximum absolute drying rate Nmax ≈ 0.197 %/min. The first derivative W'(t) was negative over the entire interval t > 0, confirming a monotonic drying curve with no local extrema within the interval.

Infrared drying kinetics

Infrared drying kinetics were investigated in five parallel series (W1-W5; Table 8, Fig. 6). Moisture content decreased from approximately 34-35% to approximately 15-16% within 240 min in all series; the Page-model nonlinearity exponent across the series was n ≈ 1.44-1.50.

Comparison of convective and infrared drying

The convective drying curve (Series B) and the mean infrared drying curve (average of series W1-W5) are compared in Fig. 7, and the corresponding comparative indices are summarized in Table 9. Infrared drying reached the same final moisture content (~15%) in half the time required by convective drying (240 versus 480 min).

Table 6. Convective drying kinetics of the pressed semi-product (Series B).

t (min)	W (%)	MR	N (%)/min
0	33.0	1.0000	-
40	32.5	0.9650	0.0125
80	31.1	0.8698	0.0350
120	29.0	0.7340	0.0525
160	27.5	0.6418	0.0375
200	26.0	0.5533	0.0375
240	24.0	0.4408	0.0500
280	21.5	0.3082	0.0625
320	19.6	0.2130	0.0475
360	17.5	0.1128	0.0525
400	16.3	0.0578	0.0300
440	15.6	0.0265	0.0175
480	15.0	0.0000	0.0150

Table 7. Statistical comparison of the Page and Fick models for Series B.

Model	RMSE	χ^2	R^2	Rating
Page	0.031	0.073	0.992	Excellent
Fick (Deff = const)	0.085	0.215	0.897	Satisfactory

Engineering heat-balance calculation for the infrared dryer

An engineering heat-balance calculation was performed for a laboratory infrared dryer using the following input data: initial mass G0 = 10 kg, W0 = 35%, Wk = 15%, t0 = 20 °C, tk = 55 °C, specific heat capacity c = 3.35 kJ/(kg × °C), latent heat of vaporization r = 2257 kJ kg^{-1}, process duration τ = 3.5 h, dryer efficiency η = 0.65.The results are given in Table 10: dry-matter mass 6.50 kg, final product mass 7.64 kg, evaporated moisture 2.36 kg, heat for product heating Q1 = 1172.5 kJ, heat for moisture evaporation Q2 = 5326.52 kJ, useful heat demand 6499.02 kJ, total heat demand (accounting for efficiency) 9998.49 kJ, required thermal power ≈1.0 kW, throughput with respect to raw material 2.86 kg h^{-1}, to finished product 2.18 kg h^{-1}, and to evaporated moisture 0.67 kg h^{-1}.

Table 8. Infrared drying kinetics of Sary Irimshik (series W1-W5).

t (min)	W1 (%)	W2 (%)	W3 (%)	W4 (%)	W5 (%)
0	35.3	34.6	34.3	34.9	34.1
20	33.8	32.0	31.3	33.0	31.0
40	31.5	29.6	28.8	30.6	28.0
60	29.0	27.0	26.5	28.0	25.3
80	26.0	24.6	24.0	25.1	23.0
100	23.5	22.0	21.5	22.7	21.0
120	21.5	20.0	19.7	20.8	19.0
140	19.7	18.2	18.0	19.0	17.4
160	18.2	17.0	16.7	17.35	16.4
180	17.1	16.2	16.0	16.65	16.2
240	16.1	15.2	15.3	15.6	15.7

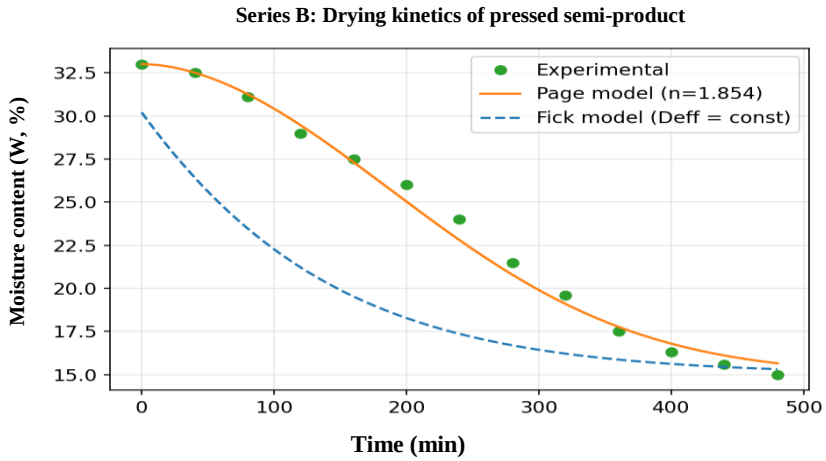

Fig. 4 Comparison of experimental data for Series B with the Page and Fick models.

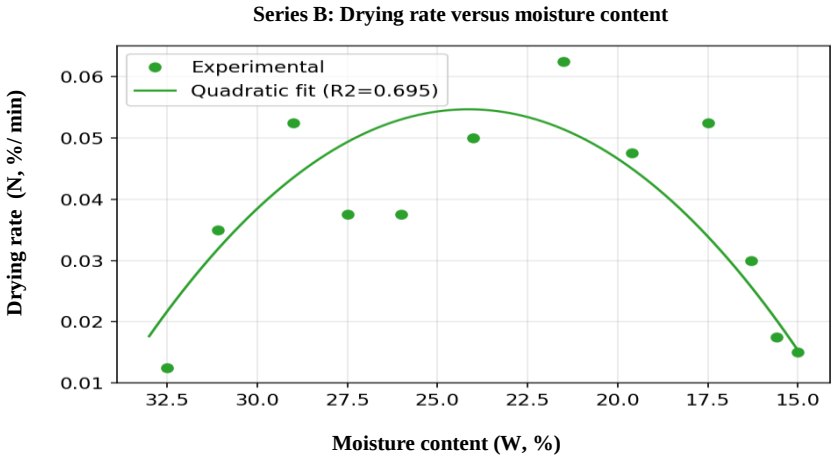

Fig. 5. Series B: drying rate as a function of moisture content, with a quadratic fit.

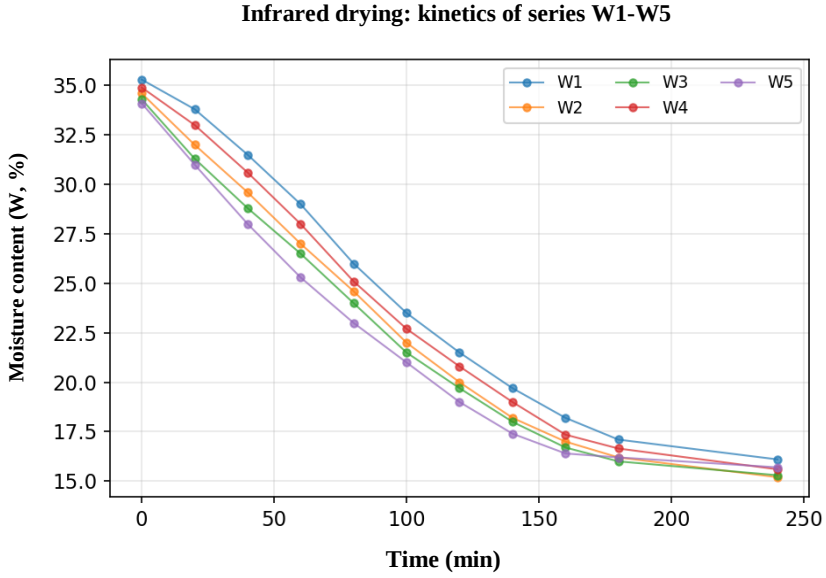

Fig. 6. Infrared drying kinetics for series W1-W5.

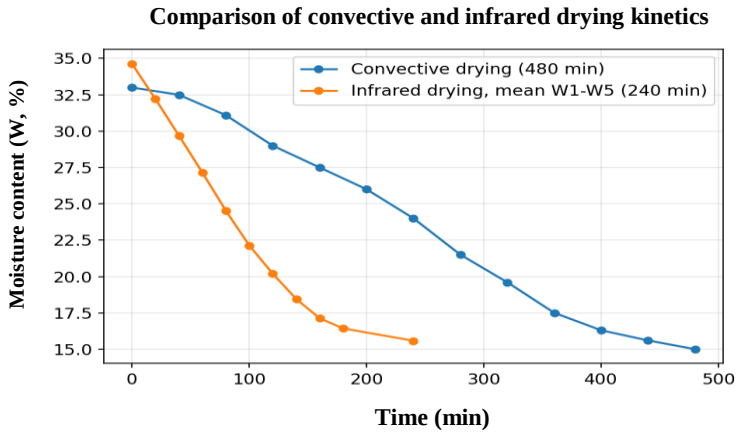

Fig. 7. Comparison of convective (Series B) and infrared (mean of series W1-W5) drying kinetics.

Table 9. Comparative indices of convective and infrared drying of Sary Irimshik.

Parameter	Convective drying	Infrared drying
Heat-transfer mechanism	Convection (heated air)	Radiant (infrared)
Temperature	50-55 °C	50-55 °C (surface); emitter 300-700 °C
Drying time (33→15%)	480 min	240 min
Page model exponent n	1.85 (semi-product) / 1.51 (raw curd)	1.44-1.50
Drying rate N	0.02-0.05 %/min	0.05-0.175 %/min
Energy consumption	Higher	20-40% lower
Crust-formation risk	Lower	Higher under an incorrect regime

Table 10. Results of the heat-balance calculation of the infrared dryer for 10 kg of Sary Irimshik.

Index	Value
Dry-matter mass (kg)	6.50
Final product mass (kg)	7.64
Evaporated moisture (kg)	2.36
Heat for product heating, Q1 (kJ)	1172.5
Heat for moisture evaporation, Q_2 (kJ)	5326.52
Useful heat demand (kJ)	6499.02
Total heat demand (with efficiency; kJ)	9998.49
Required thermal power (kW)	≈1.0 (0.79 calc.)
Throughput w.r.t. raw material (kg h^{-1})	2.86
Throughput w.r.t. finished product (kg h^{-1})	2.18
Throughput w.r.t. evaporated moisture (kg h^{-1})	0.67

DISCUSSION

The sequence in which forms of moisture become involved in dehydration (from free to adsorption-bound) is qualitatively consistent with the concept of isosteric heat of sorption, according to which the specific energy of water retention in food systems increases as weakly bound (bulk) water is exhausted and water interacting directly with protein macromolecules becomes involved (water activity and moisture sorption isotherms of food products). A similarly staged structure of moisture retention has been described for dried milk powders, in which monomolecular, polymolecular and capillary-condensed water layers with increasing binding energy are distinguished (Hardy et al. 2002). The four-component classification of moisture forms established here for Sary Irimshik therefore does not contradict, but rather specifies, the general theory of moisture binding in protein food matrices for the particular layered-porous structure of this product, which has not previously been characterized

in this detail. The final water activity obtained in this study (aw = 0.20) is well below the thresholds at which mould growth (aw ≥ 0.90) and pathogenic bacteria, including *Staphylococcus aureus* (aw = 0.94), were still recorded in model intermediate-moisture process-cheese systems; even the 'harshest' formulations previously tested, with aw = 0.81-0.86, retained microbiological stability only marginally, at the expense of sensory acceptability (Kreisman & Labuza 1978). The obtained value is also below the aw < 0.60 threshold reported as a criterion of microbiological stability for Kazakh kurt, a product of the same commodity group as Sary Irimshik (Kalibekkyzy *et al.* 2026). Consequently, the final drying moisture content of Sary Irimshik (15%, aw ≈ 0.20) provides a substantial margin of microbiological safety on storage, both confirming and refining general knowledge on the relationship between water activity and cheese-product stability for this specific object, and offering a more informative regional benchmark than comparison with Western-type cheese alone. The rising trend of moisture binding energy as aw decreases is also consistent with the general increase in isosteric heat of sorption reported for dried dairy products as a class (Hardy *et al.* 2002); no comparable quantitative binding-energy data for Sary Irimshik or structurally related products (kurut, kurt) were found in the accessible literature, underlining the novelty of the present values. The result also complements an earlier study by the same author team on the effect of enterosorbing dietary fibres on the quality and safety of fermented milk products (Alimardanova & Bakiyeva 2022): whereas safety was previously achieved through the composition of functional additives, the present work achieves a comparable reduction in water availability for microbial processes through the drying regime itself, broadening the set of tools available for ensuring the safety of fermented dairy products within this research program. The Page model provided an almost complete fit to the experimental data of Series A (R^2 = 0.9976) across the entire process, from the initial, high-moisture raw-curd stage to the equilibrium state. The nonlinearity exponent n = 1.5148 (>1) indicates a diffusion-limited process from the very beginning of drying, consistent with results reported for infrared drying of kiwifruit slices, where no constant-rate period was observed across the whole moisture range either, and the drying curve was formed entirely within the falling-rate period (Sadeghi *et al.* 2019). A similar absence of a constant-rate period, together with a satisfactory description by the Page model, was reported for convective drying of tomato slices, for which the Page model outperformed the Newton, Henderson-Pabis and logarithmic models (Agarry 2016). The wide applicability of the Page model to drying of thermosensitive plant and animal materials is further supported by studies on apricots, in which the Page model was selected as the best among 14 compared models (Menges & Ertekin 2006) and among models tested for washed dried apricots (Bozkir 2006), on golden berry (Abdulla 2012), and on foam-mat-dried kiwiberry pulp, for which the effective diffusion coefficient was likewise obtained from a Fickian diffusion approach (Bogusz *et al.* 2022). Thus, the result obtained for Sary Irimshik (absence of a constant-rate period, n > 1, high accuracy of the Page model) is not contradicted but directly corroborated by independent studies of other capillary-porous and colloidal-protein food materials, which strengthens confidence in the inferred drying mechanism. The Fick model with Deff = const systematically underestimates moisture content in the early stage and overestimates it in the late stage, which is reflected in its higher RMSE and χ^2 relative to the Page model. The local diffusion coefficient increased by almost an order of magnitude within a single experiment (from ~3.5×10^{-11} to ~3.3×10^{-10} m² s^{-1}). The absolute Deff values obtained are of the same order of magnitude as the effective diffusion coefficients reported for convectively dried tomato slices (4.43×10^{-11}-6.33×10^{-11} m² s^{-1}; Agarry 2016), and almost an order of magnitude lower than those characteristic of infrared-dried kiwifruit slices (1.2×10^{-10}-10.3×10^{-10} m² s^{-1}; Sadeghi *et al.* 2019), which is reasonable given that kiwifruit is a far less dense and more hydrated plant tissue than the dense protein-fat matrix of Sary Irimshik. The time-dependence of Deff observed here is in line with current understanding of moisture diffusion in food materials, according to which the effective diffusion coefficient is almost always dependent on the current moisture content and temperature of the material (Sadeghi *et al.* 2019); in this sense, the present result does not refute but quantitatively corroborates and refines this understanding for Sary Irimshik. The dome-shaped form of the N = f(W) curve, with a maximum at intermediate moisture content and a sharp decline at W < 20%, is typical of capillary-porous materials with volumetrically distributed resistance to moisture transfer and qualitatively resembles curves obtained for tuber and fruit-vegetable raw materials under convective and combined drying; the absolute drying-rate values (0.02-0.06 %/min) for Sary Irimshik are, however, noticeably lower than for more porous plant tissues, which is expected given the denser, more viscoelastic protein structure of the product. The analytical critical-point procedure applied here complements the conventional tabular calculation of drying rate from finite differences and allows the transition to a regime of diminishing returns in moisture removal per unit time to be identified unambiguously, without

visual inspection of the graph -- information directly applicable when deciding at what point to reduce the drying-agent temperature in order to protect thermolabile product components. The absence of a visible initial constant-rate segment in infrared drying is consistent with results for infrared-dried kiwifruit slices, where the authors explicitly report that the process proceeds entirely within the falling-rate period from the first minutes of irradiation (Sadeghi *et al.* 2019). The lower Page exponent for infrared drying (1.44-1.50) compared with convective drying of the pressed semi-product (n = 1.854) might, at first sight, be interpreted as reduced nonlinearity of the moisture-transfer mechanism. However, since two-layer thicknesses (5 and 10 mm) were tested simultaneously in the infrared series, whereas the convective series used a thinner, more uniform layer (5-7 mm), this discrepancy is more plausibly attributable to sample geometry than to a fundamental difference in the evaporation mechanism. This precludes a definitive conclusion about the effect of heating mode alone on the exponent n and is identified below as a limitation of the present study. Infrared drying reached the same final moisture content (~15%) twice as fast as convective drying (240 versus 480 min). This reduction closely matches the approximately 50% reduction in drying time previously reported for infrared drying of apples compared with convective drying (Nowak & Lewicki 2004, cited in Salehi 2020). A similar superiority of infrared drying in terms of duration, energy consumption and quality retention over convective drying was recorded in a comparative study of *Ganoderma lucidum*, in which the infrared dryer likewise reached equilibrium moisture content faster and at lower energy cost (Naseri *et al.* 2023). A synthesis of over 100 publications on infrared food drying similarly identifies shorter drying time, energy savings and higher final product quality as the principal and most consistently reproduced advantages of infrared over convective drying (Aboud *et al.* 2019). The result obtained for Sary Irimshik is therefore not a unique effect but a specific instance of a general pattern repeatedly confirmed for other food objects, which strengthens the practical recommendation formulated below. It should nonetheless be noted that the convective and infrared series in the present work were conducted on different raw-material batches and with partially different sample geometry (see above), so that the quantitative ratio of the n values should not be interpreted as an exhaustive characterization of the heating mode in isolation from the geometric factor. The specific heat consumption obtained here, $9998.49/2.36 \approx 4237$ kJ kg^{-1} (≈4.24 MJ kg^{-1}) of evaporated water, with about 82% of the total heat demand spent on evaporation, is markedly lower than the specific energy consumption reported for microwave drying of kiwi slices (7.79-16.20 MJ kg^{-1} of evaporated water, depending on power and layer thickness; Darvishi *et al.* 2016). This suggests a comparatively favorable specific energy performance of the infrared drying scheme considered here, although the comparison is necessarily indicative rather than strictly equivalent, given the difference in product nature and radiation type (infrared versus microwave).

Limitations of the study

The comparison of Page-model nonlinearity exponents for convective and infrared drying was performed on samples with partially different layer geometry (5-7 mm for convective drying versus 5 and 10 mm for infrared drying) and on different raw-material batches, which does not allow the effect of heating mode to be fully separated from the effect of layer thickness on the kinetic exponent n. A dedicated experimental series with identical sample geometry and a single raw-material source for both drying methods is required to resolve these factors unambiguously.

Engineering justification for the choice of drying method

Taken together, the results show that the layered-porous structure of Sary Irimshik substantially affects the character of dehydration: during convective drying the surface layers dry faster than the internal interlayer zones, leading to a progressive decline in moisture-transfer rate and a prolonged final stage of the process. The decrease in water activity, the increase in moisture binding energy and the decline in moisture-removal rate all indicate the development of pronounced internal resistance to mass transfer, as a result of which conventional convective drying becomes less efficient in the later stages of dehydration. Infrared or combined infrared-convective heating is therefore of technological interest for Sary Irimshik, since it provides more intensive heating of the surface and subsurface layers and accelerates moisture removal from interlayer capillary zones while simultaneously reducing specific energy consumption. This conclusion is consistent with the wider practice of applying combined infrared-convective schemes to thermosensitive and structurally heterogeneous food materials, in which volumetric infrared heating combined with convective vapour removal simultaneously intensifies the process and reduces the risk of localized surface overheating (Salehi 2020). From a practical standpoint, the kinetic models and regime parameters obtained here could in future be integrated into a digital control and optimization system for dairy-

drying production lines, an approach analogous to the application of big-data technologies for the analysis and optimization of production lines previously demonstrated by the same author team (Ussembaeva *et al.* 2025). Such integration would allow the temperature and duration of infrared drying to be adjusted in real time on the basis of the Page model, reducing both the risk of over-drying and specific energy consumption.

CONCLUSION

The layered protein-capillary porous structure of sary irimshik was established, four forms of bound moisture were identified (free, capillary-bound, osmotically bound and adsorption-bound), and their sequential involvement in dehydration was demonstrated; this classification is consistent with the general isosteric-heat-of-sorption concept applied to protein food systems.

Water activity decreased from 0.45 to 0.20 and moisture binding energy increased from 1.95 to 3.92 kJ mol^{-1} as product moisture content decreased from 33% to 15%; the resulting water activity is well below the thresholds for mould and pathogenic-bacterial growth reported for cheese-type products, confirming a high margin of microbiological stability of the finished product.

Convective drying kinetics were obtained experimentally for a raw curd (70.2 to 15.2% over 600 min) and a pressed semi-product (33.0 to 15.0% over 480 min); in both cases the process proceeded entirely within the falling-rate period, consistent with data reported for infrared-dried kiwifruit and convectively dried tomato.

Drying kinetics were adequately described by the Page model (n = 1.51-1.85; R^2 = 0.992-0.998), whereas the Fick model with a constant diffusion coefficient gave a markedly poorer fit (R^2 = 0.897) owing to the increase in Deff over time (3.5×10^{-11} to 3.3×10^{-10} m^2 s^{-1}), values of the same order as those reported for convectively dried tomato and about an order of magnitude lower than for infrared-dried kiwifruit.

Critical drying-curve parameters were determined analytically: inflection point tcr ≈ 103 min at Wcr ≈ 54% and Nmax ≈ 0.197 %/min (Series A).

Infrared drying halved the process duration (240 versus 480 min) at 20-40% lower energy consumption and a Page exponent of n ≈ 1.44-1.50; a comparable (~50%) reduction in drying time on switching to infrared heating has previously been reported for apples, *Ganoderma lucidum* and a range of other food materials, confirming the general character of this pattern.

The engineering heat-balance calculation showed that dehydration of 10 kg of sary irimshik requires an infrared-dryer thermal power of ≈1.0 kW at a throughput of 0.67 kg h^{-1} with respect to evaporated moisture and a specific heat consumption of ≈4.24 MJ kg^{-1} of moisture, which is lower than the specific energy consumption reported for microwave drying of several fruit and vegetable products.

On the basis of the combined kinetic, energetic and quality indices, infrared (or combined infrared-convective) drying is recommended as a more rational and sustainable dehydration method for sary irimshik.

REFERENCES

Abdulla, G 2012, Effect of hot air temperature on drying kinetics of golden berry.

Aboud, SA, Altemimi, AB, Al-Hilphy, ARS, Yi-Chen, L & Cacciola, F 2019, A comprehensive review on infrared heating applications in food processing. *Molecules*, 24(22): 4125.

Agarry, SE 2016, Modelling the thin-layer drying kinetics of untreated and blanch-osmotic pre-treated tomato slices. *Turkish Journal of Agriculture: Food Science and Technology*, 4(10): 850–858.

Alimardanova, MK & Bakiyeva, V 2022, Effect of enterosorbing dietary fibers on the quality and safety of fermented milk products. *Eastern-European Journal of Enterprise Technologies*, 4(11): 79–87.

Alimardanova, MK, Doumchariyeva, Zh, Zhumakhan, N, Togzhanova, K & Tlevlessova, DA 2026, Comparative kinetic modeling of ayran fermentation with functional additives. *Fermentation*, 12(7): 323.

Alimardanova, MK, Stambekova, AK, Elemesova, AA, Bayakhan, AA, Petchenko, VI & Levochkina, NA 2022, Development of the recipe, technology of a functional fermented milk product with dill greens and «Dzhusay». *BIO Web of Conferences*, 43: 03043.

Arulkumar, M *et al.* 2023, Drying kinetics, effective moisture diffusivity, and activation energy of osmotic pretreated hot-air-dried paneer cubes. *Journal of Food Processing and Preservation*, art. 7685192.

Bogusz, R, Wiktor, A, Nowacka, M, Ćwintal, J & Gondek, E 2022, Foam-mat convective drying of kiwiberry (*Actinidia arguta*) pulp. *Czech Journal of Food Sciences*, 40(3): 187–194.

Bozkir, O 2006, Thin-layer drying and mathematical modelling for washed dry apricots.

Darvishi, H, Zarein, M & Farhudi, Z 2016, Energetic and exergetic performance analysis and modeling of drying kinetics of kiwi slices.

Hardy, J *et al.* 2002, Activité de l'eau et hydratation des poudres laitières (Water activity and hydration of dairy powders). *Lait*, 82(4).

Kalibekkyzy, ZH, Zhakupbekova, Sh, Rebezov, M, Nurgazezova, A, Nurymkhan, G, Kassymov, S, Baytukenova, Sh, Mateyeva, A, Maizhanova, A & Kapshakbayeva, Z 2026, Valorization of dairy and plant by-products as functional ingredients in kurt (dried fermented milk product): Effects on nutritional, physicochemical, and sensory properties. *Foods*, 15(2): 369.

Kilic, A 2025, Comprehensive evaluation of mathematical models used in the thin-layer cold dried foods. *Food Science & Nutrition*.

Kreisman, LN & Labuza, TP 1978, Storage stability of intermediate moisture food process cheese food products. *Journal of Food Science*.

Kuzembayev, K, Kuzembayeva, GK & Tlevlessova, DA 2023, Optimization of the method of hydrothermal treatment of mogar grain for production of food concentrate “Talkan”. *Eastern-European Journal of Enterprise Technologies*, 16–25.

Menges, HO & Ertekin, C 2006, Modelling of air drying of Hachaliloglu-type apricots. *Journal of Food Engineering*.

Naseri, M, Movagharnejad, K & Nanvakenari, S 2023, Comparison of the dried properties of *Ganoderma lucidum* produced by the convective dryer and infrared dryer. *Scientific Reports*, 13: 12636.

Nassar, KS, Attia, I, Korma, SA, Ibrahim, SA, Esatbeyoglu, T & Ragab, ES 2023, Novel, functional fermented dairy product: Preparation and evaluation of dried kishk-like products from fenugreek seeds with cow's milk, camel's milk, and goat's milk. *Fermentation*, 9 (10) DOI: 10.3390/fermentation9100919

Phitakwinai, S, Thepa, S & Nilnont, W 2019, Thin-layer drying of parchment Arabica coffee by controlling temperature and relative humidity. *Food Science & Nutrition*, 7 (2), DOI: 10.1002/fsn3.1144

Sadeghi, E, Haghighi Asl, A & Movagharnejad, K 2019, Mathematical modelling of infrared-dried kiwifruit slices under natural and forced convection. *Food Science & Nutrition*, 7(11).

Salehi, F 2020, Recent applications and potential of infrared dryer systems for drying various agricultural products: A review. *International Journal of Fruit Science*.

Tastemirova, U, Mukhtarkhanova, R, Alimardanova, M, Alibekov, R & Shingisov, A 2022, Impact of vacuum freeze-drying on the reconstituted camel milk composition. *Food Science and Technology* (*Campinas*), 42: e61722. DOI: 10.1590/fst.61722.

Tuganbay, A, Yousefvand, A & Saris, PEJ 2022, Production of kurut (kurt) using probiotic *Lacticaseibacillus rhamnosus* GG strain in combination with a yeast isolated from Kazakhstan kurut. *Frontiers in Food Science and Technology*, 2: 1045579.

Zeng, Y, Liu, Y, Zhang, J, Xi, H & Duan, X 2019, Effects of far-infrared radiation temperature on drying characteristics, water status, microstructure and quality of kiwifruit slices.

Bibliographic information of this paper for citing:

Alimardanova, M, Kuzembayev, K, Kuzembayeva, G, Tlevlessova, D 2026, Sustainable dehydration of Sary Irimshik, a layered-porous fermented dairy product: Comparative kinetics and energy efficiency of convective and infrared drying, Caspian Journal of Environmental Sciences, 24: 1177-1189.

Copyright © 2026